

# Effect of platinum distribution on the hydrogen gas sensor properties in tin oxide thin films

TAKEYUKI SUZUKI, TSUTOMU YAMAZAKI, KAZUYUKI TAKAHASHI,  
TADASHI YOKOI

*Department of Industrial Chemistry, Tokyo University of Agriculture and Technology, Koganei,  
Tokyo 184, Japan*

Tin oxide and platinum layers were deposited on oxidized silicon wafers by ion-beam sputtering. The hydrogen gas sensing properties of undoped films and platinum-doped films were examined at 300° C for films annealed at 500° C. It was observed that the surface platinum when annealed together with the tin oxide film increased the sensitivity and reduced the response time compared with those of undoped films. Longer annealing tended to shift the optimum sensor thickness to a thicker side; the optimum thickness changed from 17 to 37 nm as the annealing time increased from 2 to 50 h. The interdiffusivity between the platinum and the tin atoms in the bulk was negligibly small at 300° C.

## 1. Introduction

The addition of a small amount of metals, such as silver, palladium and platinum, to the tin oxide sensors is known to enhance the sensitivity to combustible gases and toxic gases [1-4]. These metals are usually distributed homogeneously in the tin oxide matrix through mixing and sintering. However, the homogeneous distribution of dopants is not an a priori requisite for a better sensor property. In fact, doping of precious metals on the free surface of tin oxide is reported to improve the sensor characteristics. For example, McAleer *et al.* [5] have surface-treated the porous tin oxide with platinum and palladium by immersion in an aqueous solution followed by drying and thermal deposition. They found that both the resistivity in air and the gas response are modified. Kuriki *et al.* [6] have sputter-deposited a platinum layer 2 nm thick on the surface of the 30 nm thick tin oxide film at 300° C. The response measurements of the film showed an enhanced sensitivity to ethanol, carbon monoxide and hydrogen gases; SEM observation revealed a dispersion of the island-structured platinum of ~ 30 nm in size instead of a designed 2 nm layer.

These observations prompted a further study of the influence of platinum distribution on the sensor properties so that the resulting films may show an improved gas response.

In this paper, we describe the different types of platinum distribution, their influence on the hydrogen sensing and the platinum diffusion in the film. Thickness dependence of the sensor property is also described, because our previous studies [7, 8] have demonstrated the existence of an optimum film thickness.

## 2. Experimental methods

Films were deposited through a sputter mask on to

oxidized silicon wafers (4 mm × 8 mm); oxidation was done by heating the silicon wafers at 900° C for 1 h in air in an electric furnace. Deposition was carried out by ion-beam sputtering (IBS) from a target of 99.99% pure SnO<sub>2</sub> (High Purity Chemical Lab.) and of platinum plate. Details of the IBS apparatus have been published elsewhere [9, 10].

Sample configurations with different platinum distributions are shown schematically in Fig. 1. They are undoped films of varying thickness (Fig. 1a), a thin layer of platinum dispersed on the surface (Fig. 1b), a rectangular platinum bar (0.47 mm wide, 60 nm thick and 4 mm long) parallel to the electrode (Fig. 1c), one layer of platinum in the middle of the film (Fig. 1d) and equidistant four layers of platinum in the film (Fig. 1e). The thickness of the platinum electrode was always 60 nm and the electrode gap was 0.4 mm except for the configuration depicted in Fig. 1c where the gap was 2.45 mm.

The total film thickness and thus the deposition rate was measured first with a surface texture measuring instrument (Ferfcom, Tokyo Precision) for undoped tin oxide and platinum films and then calculated from the low-angle X-ray diffraction (XRD) peaks of the multilayered films composed of Ag/SnO<sub>2</sub> and Ag/Pt. A desired layer thickness was achieved by a controlled sputtering time using the deposition rate thus determined. XRD was taken with a 30 kV-20 mA nickel-filtered CuK $\alpha$  radiation (RAD-B, Rigaku). The low-angle X-ray intensity data were collected with a scan speed of 0.2° min<sup>-1</sup> and a step sampling of 0.004° in 2 $\theta$ . Deposited films were annealed in air in an electric furnace and their sensor properties at 300° C were measured and recorded on a chart. The gas response was obtained from the change in the output voltage,  $V_x$ , in Fig. 2 when the synthetic-air (s-air) was replaced by the 0.47% hydrogen gas and s-air or vice versa. The flow rate of both gases were set to 50 ml min<sup>-1</sup>. As

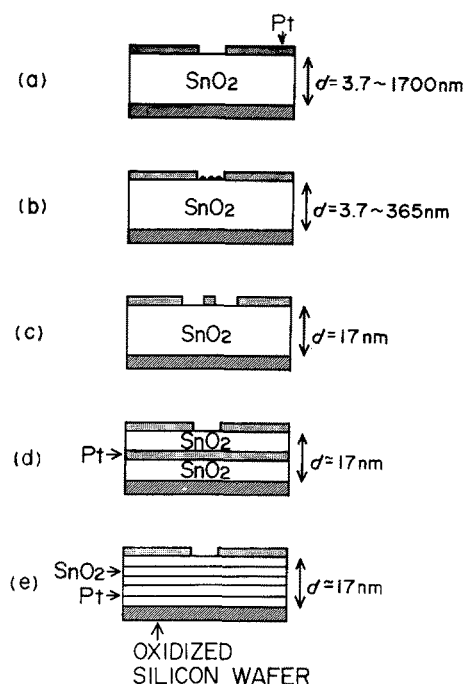


Figure 1 Five sample configurations with different platinum distributions.

shown in the figure, the sensor resistance,  $R_s$ , is determined from a variable d.c. voltage,  $V_0$ , and a standard resistance,  $R_x$ .  $V_0$  was adjusted so that the current density in s-air lay between  $\sim 0.1$  and  $1 \text{ A cm}^{-2}$ . The sensitivity was defined as the ratio of the film resistance in s-air ( $R_0$ ) to that in 0.47% hydrogen gas ( $R_g$ ).

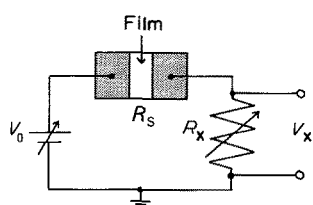
### 3. Results and discussion

#### 3.1. Film structure

Fig. 3 shows the XRD diagram of the substrate and the 200 nm thick tin oxide film before and after annealing. The substrate shows a small reflection from the silicon dioxide (marked  $\Delta$ ) and a strong peak from the silicon (400) plane; a small peak at  $2\theta \sim 62.5^\circ$  is due to the remaining  $\text{CuK}\beta$  reflection from the silicon (400) plane. As-deposited film shows only broad haloes indicating amorphous or microcrystalline nature of the film. Annealed film has a tetragonal structure (marked  $\circ$ : JCPDS 21-1250) with increased reflection intensity from the silicon dioxide. Longer annealing made the intensity from the tin oxide sharper, indicating the growth of the crystallites; however annealing induced no preferred grain growth.

#### 3.2. Undoped-film

The thickness dependence of sensor properties in undoped tin oxide films were examined first for films



$$R_s = \left( \frac{V_0}{V_x} - 1 \right) R_x$$

Figure 2 Measurement circuit for sensor properties.

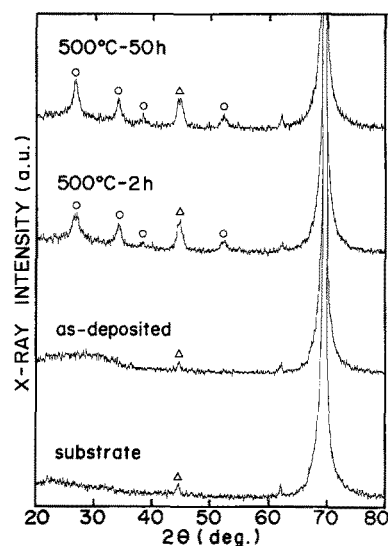


Figure 3 X-ray diffraction diagram of substrate (oxidized silicon wafer), as-deposited tin oxide film and annealed tin oxide film. The thickness of the tin oxide film is 200 nm. ( $\circ$ ) Tin oxide, ( $\Delta$ ) silica.

with as-deposited thickness of 3.7, 7.9, 17, 37, 79, 170, 365, 788 and 1700 nm. These films were annealed at  $500^\circ\text{C}$  for 2 h to study the sensor characteristics. Fig. 4 shows the sensitivity and resistance of these films as a function of thickness. As shown clearly, the 17 nm film exhibits a markedly high sensitivity compared with other films; films thinner than  $\sim 5$  nm and thicker than  $\sim 30$  nm are almost insensitive. This thickness dependence of sensitivity is similar to the reported behaviour of amorphous films at  $150^\circ\text{C}$  and polycrystalline films (annealed  $500^\circ\text{C}$ -2 h) at 150 and  $250^\circ\text{C}$ , but different from polycrystalline films at  $350^\circ\text{C}$  on sintered alumina substrates [7, 8]. The former are sensitive at the thinner side ( $\sim 5$  to  $\sim 20$  nm) and the latter at the thicker side ( $\sim 20$  to  $\sim 150$  nm); polycrystalline films at  $300^\circ\text{C}$  show both characteristics and are sensitive both at  $\sim 6$  nm and at  $\sim 40$  to  $\sim 100$  nm. It should be noted that it has only been possible to measure these sensor properties having an electrode gap of  $\sim 0.4$  mm for films thicker than  $\sim 5$  nm because of the high resistance in thinner films on alumina. On the other hand, the resistivity of polycrystalline films prepared as reported here on oxidized

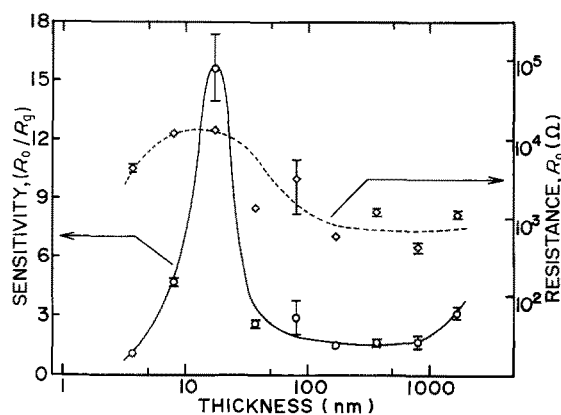


Figure 4 The thickness dependence of sensitivity and resistance in undoped films annealed at  $500^\circ\text{C}$  for 2 h in air. The thickness from left to right is 3.7, 7.9, 17, 37, 79, 170, 365, 788 and 1700 nm, respectively. Sensor properties are measured at  $300^\circ\text{C}$ .

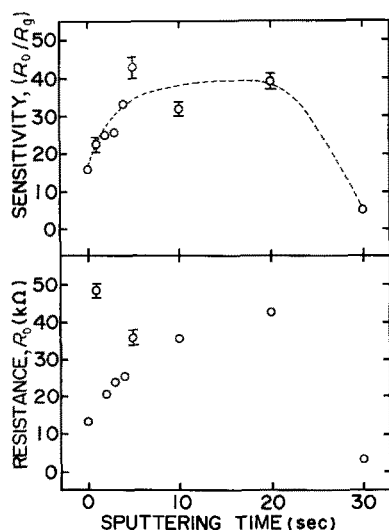


Figure 5 Sensitivity and resistance at 300°C in 17 nm films with surface platinum deposited up to 30 sec. Deposition rate of platinum  $\sim 0.03 \text{ nm sec}^{-1}$ . Films are annealed at 500°C for 50 h together with the surface platinum.

silicon are always lower by several orders of magnitude than that on alumina, fused silica, Pyrex, mullite and magnesia [8].

Thus, for an undoped-film sensor, an oxidized silicon wafer is preferable to other substrates, because it provides films with a low resistance of the order of 10 kΩ. This may be due to the surface smoothness and the thermal expansion coefficient of the silica layer on the silicon wafer.

### 3.3. Platinum on the surface

The effect of platinum distribution on the surface of the 17 nm film (Fig. 1b) was examined next. The layer thickness of platinum was varied to determine the optimum thickness; platinum was sputtered from 1 to 5 sec at 1 sec intervals and for 10, 20 and 30 sec. With a deposition rate of platinum of  $\sim 0.03 \text{ nm sec}^{-1}$ , the sputtering layer thickness ranged from  $\sim 0.03$  to  $\sim 0.9 \text{ nm}$ . As the platinum atomic radius is 0.139 nm, the platinum distribution tested corresponds to thicknesses from an isolated island structure to approximately 3 layers. These 17 nm films were annealed

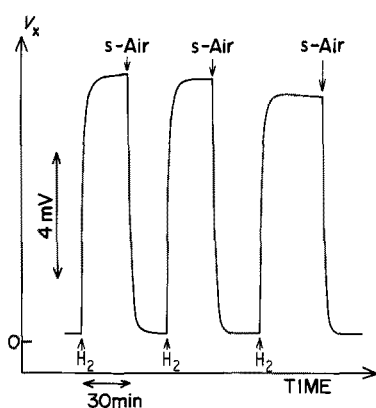


Figure 6 Response curve of the 17 nm film with surface platinum deposited for 5 sec. Film is annealed at 500°C for 50 h together with the surface platinum and the response is measured at 300°C. Deposition rate of the platinum is  $\sim 0.03 \text{ nm sec}^{-1}$ .  $V_0 = 22 \text{ mV}$ ,  $R_x = 0.5 \text{ k}\Omega$ .

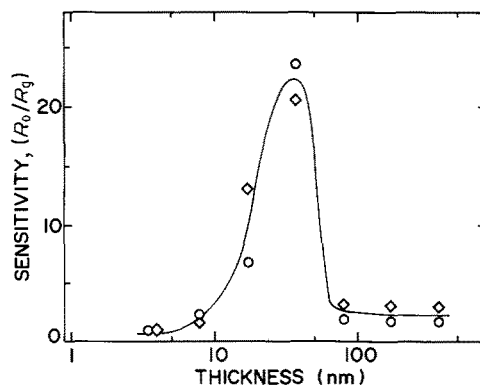


Figure 7 Thickness dependence of sensitivity in (O) undoped and ( $\diamond$ ) platinum-doped (5 sec) films annealed at 500°C for 50 h. Platinum is deposited after annealing the films; platinum is not annealed at 500°C, but is heat-treated at 300°C during measurement of the sensor properties. The thickness from left to right is 3.7, 7.8, 17, 37, 78, 170 and 365 nm, respectively.

together with the surface platinum at 500°C for 50 h and served as sensors. Fig. 5 shows the sensitivity and resistance as a function of sputtering time. The sensitivity increased up to  $\sim 40$  with increasing platinum thickness from  $\sim 0.1$  to 0.5 layers; naturally platinum is dispersed on the surface as islands. From  $\sim 0.5$  to  $\sim 2$  layers (20 sec), the films exhibited a highly sensitive plateau and then the sensitivity decreased down to  $\sim 5$  with  $\sim 3$  layers (30 sec). The drop in resistance down to 3.3 kΩ at  $\sim 3$  layers indicates that surface platinum is distributed so that it became electrically continuous at least at  $\sim 3$  layers. Another interesting feature is that resistance in s-air generally increased with platinum thickness up to  $\sim 2$  layers. It may be that the catalytic effect of platinum enhanced oxygen adsorption which resulted in a higher resistance. As an example of this series of surface platinum, the response curve of the 17 nm film with an optimum platinum distribution, 5 sec sputtering and 500°C–50 h annealing, is shown in Fig. 6. The time needed to attain a sensitivity of 10 was  $\sim 30$  sec, shorter than the corresponding 60 to 120 sec of the undoped 17 nm film annealed at 500°C for 2 h.

The next experiment was aimed to examine if the optimum thickness (17 nm) still holds under longer annealing (500°C–50 h) and if the platinum annealing, together with the tin oxide film, is necessary for a better sensor operation. Fig. 7 shows the thickness dependence of sensitivity in undoped tin oxide films annealed at 500°C for 50 h and that of as-deposited platinum on the surface. The sputtering time of platinum was 5 sec ( $\sim 0.5$  layer). It is evident that the sensitivity maximum of the undoped film shifted towards the thicker side. The 37 nm film showed a sensitivity of  $\sim 24$  whereas that of the 17 nm film fell to 7; those of other films are less than 3. The results also show that the as-deposited platinum does not necessarily improve the sensitivity; both undoped and doped films exhibited almost the same thickness dependence of sensitivity.

Fig. 8 shows the response curves of the optimum 37 nm films with (b) and without (a) platinum. A comparison of the curves shows that the film with as-deposited platinum responds to hydrogen gas more

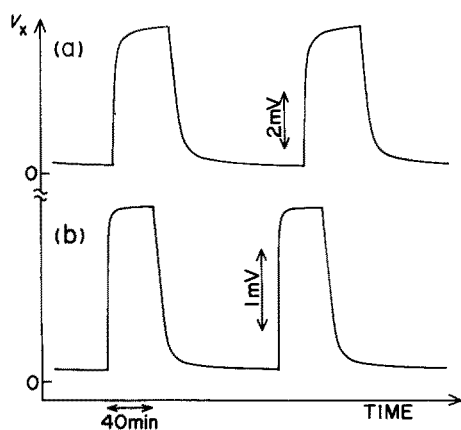


Figure 8 Response curve of the 37 nm films (a) without and (b) with the surface platinum. Platinum is deposited for 5 sec at a deposition rate of  $\sim 0.03 \text{ nm sec}^{-1}$ . Films are annealed at  $500^\circ\text{C}$  for 50 h and the platinum is deposited on to the annealed film. The response curve is measured at  $300^\circ\text{C}$ . (a)  $V_0 = 15 \text{ mV}$ ,  $R_x = 0.2 \text{ k}\Omega$ . (b)  $V_0 = 7 \text{ mV}$ ,  $R_x = 0.2 \text{ k}\Omega$ .

rapidly than the undoped-film. The response time for a sensitivity of 10 was  $\sim 60 \text{ sec}$  in the pure film and 40 to 50 sec in the platinum-dispersed film. These results show that the optimum thickness changes with annealing and that annealing the surface platinum together with the film improves the sensor properties.

Thus far we have been concerned with the sensor configuration depicted in Figs 1a and b. Let us now examine the configuration shown in Fig. 1c. A platinum bar was deposited in the middle of the electrode gap and annealed at  $500^\circ\text{C}$  for 50 h together with the 17 nm film. A comparative test of the sensors with and without the platinum bar showed that the platinum bar decreased the electrical resistance to one-quarter and the sensitivity to one-half. Thus we see that a thick platinum layer plays no important role in improving the sensor properties; it merely works as an electric conductor.

### 3.4. Platinum in the film

In a previous work [8], we have postulated that the depletion region just beneath a grain boundary is deeper compared to other homogeneous surfaces, thus leading to the formation of an uneven depletion region. The configuration shown in Figs 1d and e was made to study if one can obtain a flat depletion layer parallel to the surface so that one may improve the sensor characteristics.

As the first trial, one platinum layer was deposited in the middle of the 17 nm film from 1 sec ( $\sim 0.1$  layer) to 11 sec ( $\sim 1.2$  layers) at each 2 sec ( $\sim 0.2$  layer) interval (Fig. 1d). These films were annealed at  $500^\circ\text{C}$  for 2 h; this increased the resistance up to 7 sec ( $\sim 0.8$  layer) and decreased it above 9 sec ( $\sim 1$  layer). However, no clear correlation was observed between the sensitivity and the platinum layer thickness below  $\sim 0.8$  layer; the sensor became almost insensitive above  $\sim 1$  layer. The last configuration (Fig. 1e) consists of four layers of platinum in the 17 nm film; platinum thickness was  $\sim 0.1$  layer (1 sec). This increased the resistance but the sensitivity remained almost unchanged. The role of dispersed platinum in the tin oxide film is yet to be solved.

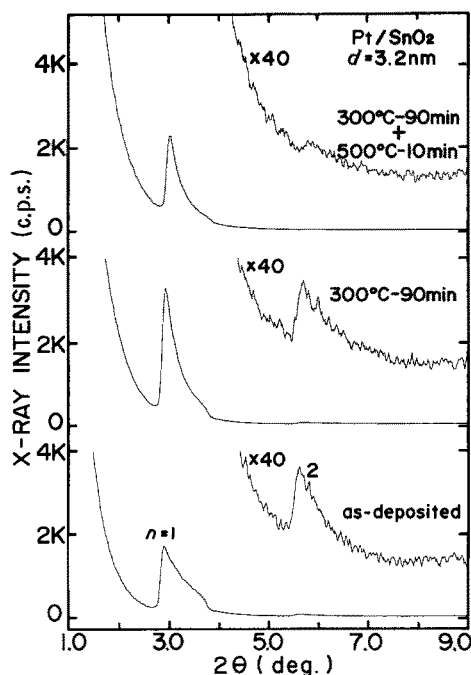


Figure 9 X-ray diffraction diagrams of Pt/SnO<sub>2</sub> multilayered film fabricated as Pt ( $\sim 0.03 \text{ nm}$ )/SnO<sub>2</sub> (3.2 nm)  $\times$  30 pairs.

### 3.5. Diffusion of platinum

Knowledge of platinum diffusion, leaving aside the catalytic action, in a porous sintered body [2, 3] or in a thin film, is necessary to discuss the sensor stability.

In a previous work [11], we reported an interdiffusivity as low as  $9 \times 10^{-22} \text{ cm}^2 \text{ sec}^{-1}$  at  $500^\circ\text{C}$  in multilayered films of Pt/SnO<sub>2</sub> with an interplanar distance  $d = 3.5 \text{ nm}$ . The method, as proposed by Dumond and Youtz [12], consists of relating the interdiffusivity,  $\tilde{D}_d$ , to the decay rate of the integrated X-ray intensity  $I(t)$

$$\tilde{D}_d = - \frac{\log_e [I(t_0)/I(t)]}{8\pi^2(t - t_0)} d^2 \quad (1)$$

where  $t$  is the time. Because the scattering factor of the platinum is larger than that of the tin atom, the interdiffusivity thus obtained represents an approximate value of the platinum diffusivity.

Here, the diffusivity of platinum in a low platinum concentration interests us. Thus multilayered films of Pt ( $\sim 0.03 \text{ nm}$ )/SnO<sub>2</sub> (3.2 nm)  $\times$  30 pairs were fabricated; platinum was sputtered for 1 sec forming a thickness of  $\sim 0.1$  layer. Fig. 9 shows the low-angle diffraction diagram of an as-deposited and annealed film. It is surprising that distantly dispersed platinum atoms,  $\sim 1 \text{ nm}$  apart in a plane, present a Bragg reflection of  $2d \sin \theta = n\lambda$ , where  $n$  is the order of reflection and  $\lambda$  is the X-ray wavelength (0.154 nm). As-deposited film showed  $n = 1$  and 2 reflections and the  $n = 2$  reflection almost vanished when annealed at  $500^\circ\text{C}$  for 10 min.

Fig. 10 shows the decay rate of the integrated X-ray intensity; annealing at  $300^\circ\text{C}$  changed the intensity little. According to Equation 1, the decay rate of  $500^\circ\text{C}$  gives an approximate platinum diffusivity and thus the diffusivity of  $(4.2 \pm 0.7) \times 10^{-19} \text{ cm}^2 \text{ sec}^{-1}$  was calculated using the least square method. Similarly, the decay rate during long annealing (352 h) of Pt

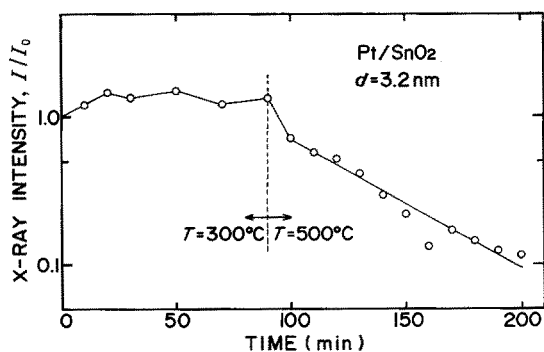


Figure 10 The decay rate of the integrated  $n = 1$  X-ray intensity relative to the as-deposited intensity. Annealing at  $500^\circ\text{C}$  induces the interdiffusion in the multilayered film.

(0.9 nm)/SnO<sub>2</sub> (2.6 nm)  $\times$  31 pairs at  $500^\circ\text{C}$  gave  $(8.9 \pm 0.8) \times 10^{-22} \text{ cm}^2 \text{ sec}^{-1}$ , which is practically the same value with  $9 \times 10^{-22} \text{ cm}^2 \text{ sec}^{-1}$  obtained from the shorter annealing time for 96 h [11].

These low values of platinum diffusivity at  $500^\circ\text{C}$ , together with an almost invariant X-ray intensity with time at  $300^\circ\text{C}$ , demonstrate that the doped platinum helps immobilize the constituent atoms in the bulk at the sensor-operating temperature of  $\sim 300^\circ\text{C}$ .

#### 4. Conclusions

Tin oxide films and platinum layers were deposited on to oxidized silicon wafers by the ion-beam sputtering. Their sensor properties at  $300^\circ\text{C}$  against 0.47% hydrogen gas and the interdiffusion at  $500^\circ\text{C}$  in the platinum/tin oxide multilayered films were examined.

1. The 17 nm thick undoped-film showed a sensitivity of  $\sim 15$  when annealed at  $500^\circ\text{C}$  for 2 h in air. No other films between 3.7 and 1700 nm thick showed such a high sensitivity; the sensitivities were less than  $\sim 5$ .

2. The 17 nm film with surface platinum of average thickness between 0.15 and 0.6 nm exhibited a high sensitivity ( $\sim 30$  to  $\sim 40$ ) when the films were annealed at  $500^\circ\text{C}$  for 50 h together with the surface platinum.

3. The sensitivity maximum of the undoped-films shifted towards a thicker side when annealed at  $500^\circ\text{C}$  for 50 h; the 37 nm film showed a sensitivity of  $\sim 24$  whereas that of the 17 nm film fall to 7; those of other films were less than 3.

4. An as-deposited platinum layer ( $\sim 0.15$  nm thick) on the annealed films ( $500^\circ\text{C}$ -50 h) made the response time shorter; however, this platinum layer did not necessarily increase the sensitivity.

5. The interdiffusivity in multilayered films at  $500^\circ\text{C}$  was  $(4.2 \pm 0.7) \times 10^{-19}$  and  $(8.9 \pm 0.8) \times 10^{-22} \text{ cm}^2 \text{ sec}^{-1}$  for Pt ( $\sim 0.03$  nm)/SnO<sub>2</sub> (3.2 nm)  $\times$  30 pairs and Pt (0.9 nm)/SnO<sub>2</sub> (2.6 nm)  $\times$  31 pairs, respectively.

#### Acknowledgement

We thank Professor N. Oyama of the Department of Applied Chemistry for Resources for help in film thickness analysis.

#### References

1. K. MURAKAMI, S. YASUNAGA, S. SUNAHARA and K. IHOKURA, in "Proceedings of the International Meeting on Chemical Sensors", Fukuoka, September 1983, edited by T. Seiyama, K. Fueki, J. Shiokawa and S. Suzuki (Elsevier, Kodansha, 1983) p. 18.
2. Y. MATSUURA, N. MURAKAMI and K. IHOKURA, *ibid.*, p. 24.
3. Y. OKAYAMA, H. FUKAYA, K. KOJIMA, Y. TERASAWA and T. HANDA, *ibid.*, p. 29.
4. N. YAMAZOE, Y. KUROKAWA and T. SEIYAMA, *ibid.*, p. 35.
5. J. F. McALEER, P. T. MOSELEY, J. O. W. NORRIS, D. E. WILLIAMS and B. C. TOFIELD, in "Proceedings of the 2nd International Meeting on Chemical Sensors", Bordeaux, July 1986, edited by J.L. Aucoutrier, L.S. Cauhapé, M. Destriau, P. Hagenmuller, C. Lucat, F. Ménil, J. Portier and J. Salardenne (University of Bordeaux, 1986) p. 264.
6. S. KURIKI, K. SANO, H. KONISHI and G. MATSUMOTO, *Denshi Tsuushin Gakkai Ronbun-shi '86/6 J69-C* (1986) 754.
7. T. SUZUKI, T. YAMAZAKI, H. YOSHIOKA and K. HIKICHI, *J. Mater. Sci.* **23** (1988) 145.
8. *Idem, ibid.*, **23** (1988) 1106.
9. T. SUZUKI, T. YAMAZAKI, H. YOSHIOKA, K. TAKAHASHI and T. KAGEYAMA, *J. Mater. Sci. Lett.* **6** (1987) 437.
10. T. SUZUKI, T. YAMAZAKI, K. TAKAHASHI, T. KAGEYAMA and H. ODA, *ibid.*, **7** (1988) 79.
11. T. SUZUKI, T. YAMAZAKI and T. YOKOI, *ibid.*, **7** (1988) 669.
12. J. DUMOND and J. P. YOUTZ, *J. Appl. Phys.* **11** (1940) 357.

Received 7 April  
and accepted 5 September 1988